A high sensitivity localized surface plasmon resonance sensor based on D-shaped photonic crystal fiber for low refractive index detection*

PAN Honggang, CAO Chuanbo, ZHANG Ailing, PAN Fei, SUI Pengxia, and LIU Xinbo**

Engineering Research Center of Optoelectronic Devices and Communication Technology, Ministry of Education, Tianjin Key Laboratory of Thin Film Electronics and Communication Devices, School of Integrated Circuit Science and Engineering, Tianjin University of Technology, Tianjin 300384, China

(Received 23 December 2021; Revised 16 March 2022)

In this paper, a localized surface plasmon resonance (LSPR) refractive index sensor based on photonic crystal fiber (PCF) is proposed to solve the problem of low refractive index analyte detection. 31 silver nanowires are placed on the surface of the D-shaped PCF, which increases the contact area between the plasma material and the analyte. The simulation results indicate that the maximum sensitivity of the sensor reaches 16 400 nm/RIU, and the refractive index detection range is 1.26—1.33. It is proved that the sensor has a good prospect in low refractive index detection.

Document code: A **Article ID:** 1673-1905(2022)07-0425-5

DOI https://doi.org/10.1007/s11801-022-1193-8

In recent years, the method of surface plasmon resonance (SPR) effect for refractive index sensing has been widely used in biology, medicine, chemistry and other fields[1]. Since the concept of photonic crystal was proposed in 1987, photonic crystal fiber (PCF) has gradually entered the vision of scientists. Due to its good transmission characteristics, it is mostly used in the sensing field. At present, there are more and more methods to measure the refractive index of analytes through PCF sensing[2]. However, it is difficult to fill the air holes with liquid, which greatly limits the practical applications[3]. In order to solve the problems above, a side-polished PCF is proposed, which facilitates immersion in different analytes for measurement[4]. And this technology makes it possible to fill PCF with a single kind of metal nanoparticles[5], with which the evanescent field of guided mode can couple and excite the localized surface plasmon resonance (LSPR) around the surface of metal nanoparticles[6]. Compared with ordinary SPR sensor, the LSPR sensor has larger contact area between plasma material and liquid for measurement, which can realize micro-liquid detection. What's more, the use of nanowires or nanoparticles is much easier than depositing metal film.

In the proposed sensor structure, the commonly used plasma materials are gold or silver. Using silver materials can obtain sharper loss peaks and higher detection accuracy. In LSPR sensors, nanowires are often used. FU et al[7] placed graphene coated silver nanocolumns on the surface of D-shaped single-mode fiber to obtain the maximum sensitivity of 8 860.93 nm/RIU, and the refractive index detection range is 1.33—1.39. WANG et al[8] selectively filled the air holes of PCF with gold nanowires, realizing an ultra-wide refractive index detection range of 1.29—1.49. However, when the refractive index of the analyte is lower than 1.33, the sensitivity is only 2 500 nm/RIU. In the detection of low refractive index analytes, the reported researches have the problem of low sensitivity. ZHANG et al[9] plated a nano gold band on the surface of D-shaped PCF and obtained a refractive index detection range of 1.2—1.4, with a maximum sensitivity of 3 710 nm/RIU. LIU et al[10] proposed a dual channel SPR sensor with resonance wavelength in the mid infrared region, and obtained a sensitivity of 5 500 nm/RIU when the refractive index of the analyte was 1.23—1.29. To sum up, most of the proposed sensing structures can only detect analytes with refractive index higher than 1.33, while the detection of analytes with refractive index lower than 1.33 still has low sensitivity.

This paper proposed a structure of placing 31 silver nanowires on the surface of D-shaped PCF. The maximum sensitivity of 16 400 nm/RIU is simulated through COMSOL Multiphysics, and the detection range is achieved from 1.26 to 1.33. Compared with Refs.[8—10], this structure obtains higher sensitivity in the measurement of low refractive index analyte. At present, the refractive index of some medical reagents is lower than 1.33.

* This work has been supported by the Key Project of Tianjin Natural Science Foundation (No.20JCZDJC00500), and the Tianjin Postgraduate Research and Innovation (No.2020YJSS009).
** E-mail: alzhang@email.tjut.edu.cn

For example, the refractive index of sevoflurane is about 1.27, which can be used as anesthetics in the medical field. Therefore, our research may have potential applications in drug detection and drug leakage monitoring.

The sensor structure profile proposed is shown in Fig.1. The silver nanowires are placed on the surface of the D-shaped PCF, the air holes are arranged in a non-regular hexagonal shape, and the air hole diameter is d_1=1.3 μm. The pitches of adjacent air holes are labelled by Λ_1=4 μm and Λ_2=2.5 μm. The distance H=3.2 μm is from the fiber center to the polished surface. The spacing of silver nanowires is Λ_3=40 nm and the diameter is d_2=120 nm.

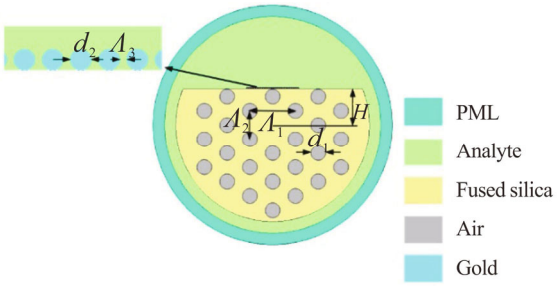

Fig.1 Cross section of the proposed sensor

The background material of optical fiber is fused silica, and the change of material dispersion with wavelength is determined by Sellmeier equation[11] as

$$n^2-1=\frac{0.696\,166\,3\lambda^2}{\lambda^2-(0.068\,404\,3)^2}+\frac{0.407\,942\,6\lambda^2}{\lambda^2-(0.116\,241\,4)^2}+\frac{0.847\,479\,4\lambda^2}{\lambda^2-(9.896\,161)^2}, \tag{1}$$

where λ is the wavelength of incident light.

Silver nanowires are selected as the plasma material, and the dielectric constant of silver can be calculated by

$$\varepsilon_m(\lambda)=\varepsilon_{mr}+i\varepsilon_{mi}=1-\frac{\lambda^2\lambda_c}{\lambda^2{}_p(\lambda_c+i\lambda)}, \tag{2}$$

where λ_p and λ_c represent the plasma wavelength and collision wavelength, respectively. The parameter values are obtained from Ref.[12].

The parameter of confinement loss is usually introduced into the analysis of the sensor. The confinement loss of sensor can be expressed as[13]

$$\alpha_{loss}=8.686\times\frac{2\pi}{\lambda}\mathrm{Im}(n_{eff})\times10^4\ \ (\mathrm{dB/cm}), \tag{3}$$

where λ is the wavelength of the incident light and Im(n_{eff}) is the imaginary part of the effective refractive index.

Fig.2(a) shows the mode dispersion when the refractive index of the analyte is 1.31. The meaning of each curve is given in the legend. The imaginary part of the effective refractive index of the fundamental mode decreases gradually after reaching the peak. This peak point is called the phase matching point. Fig.2(b) shows the optical field distribution of the fundamental mode. Fig.2(c) shows the optical field distribution of the fundamental mode at resonance wavelength. It can be concluded that when the two modes are strongly coupled, the energy transferring from the fundamental mode to the plasmonic mode is the largest.

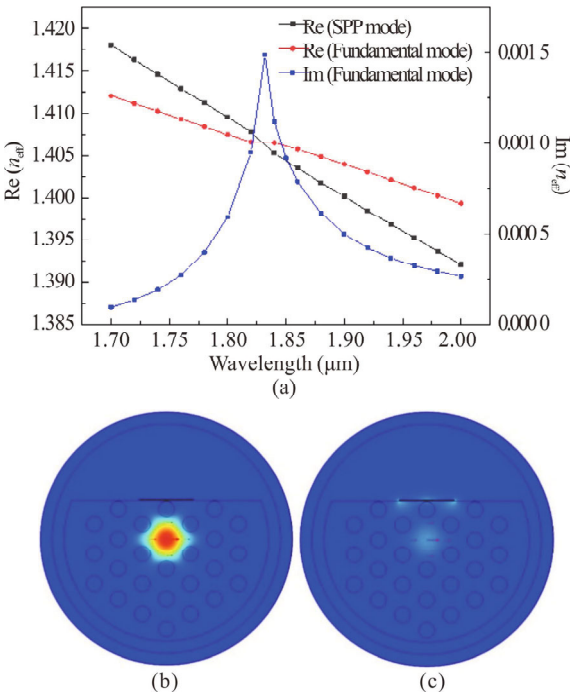

Fig.2 (a) Mode dispersion comparison diagram; (b) Optical field distribution (fundamental mode); (c) Optical field distribution of the fundamental mode at resonance wavelength

In LSPR sensors, wavelength sensitivity and full width at half maximum (*FWHM*) are two important parameters to measure the performance of the sensor. The figure of merit (*FOM*) is defined as the ratio of wavelength sensitivity to *FWHM*, which is another important parameter. Its expression is[14]

$$FOM=\frac{S}{FWHM}, \tag{4}$$

where S is the wavelength sensitivity of the sensor. It can be seen from Eq.(4) that the larger sensitivity and the smaller *FWHM* will make the *FOM* larger and the better performance of the sensor.

The number of silver nanowires will affect the resonance wavelength by changing the contact area. In Fig.3, n is the number of nanowires, n_a is the refractive index of the analyte, the solid line is the formant when the refractive index of the analyte is 1.31, and the dotted line is the formant when the refractive index of the analyte is 1.32. It can be seen from Fig.3 that when the number of nanowires is 31, the confinement loss is the largest and the sensitivity is higher. The main reason why the other two numbers of nanowires will reduce the loss may be that when the number of nanowires becomes less, the energy leaked from the core mode is not fully absorbed by the plasma material. And when the number of

nanowires increases, the main reason for the decrease of sensitivity is that the energy coupling between nanowires will affect the occurrence of SPR effect.

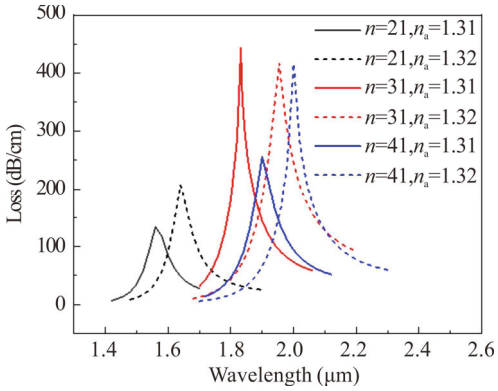

Fig.3 Variation of loss peak with the number of silver nanowires at n_a=1.31 and 1.32

As we all know, all structural parameters will affect the effective refractive index of the PCF and then result in blue shift or red shift of the resonance wavelength. Fig.4 shows the variation of loss peak with different air hole diameters. In Fig.4, when the air hole diameter is 1.3 μm, the confinement loss is higher than that with the diameter of 1.4 μm, and the *FWHM* is narrower than that with the diameter of 1.2 μm, so the diameter of 1.3 μm is selected for this sensor.

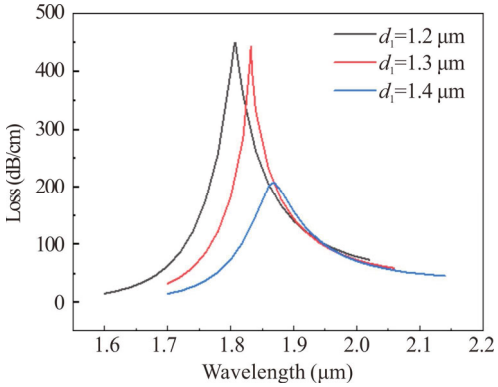

Fig.4 Variation of loss peak with the air hole diameter

Fig.5(a) shows the comparison of loss peaks between regular hexagonal air holes and non-regular hexagonal air holes. Fig.5(b) shows the arrangement structure of regular hexagonal air holes. It can be seen from Fig.5(a) that when the air holes are arranged in non-regular hexagonal structure, the resonance wavelength presents an obvious blue shift, and its *FWHM* is narrower, so the *FOM* becomes larger, leading to better sensor performance.

Fig.6(a) shows the influence of different nanowire diameters on resonance peak. It can be seen that when the nanowire diameter is 120 nm, we get narrower *FWHM* and higher confinement loss than those with the nanowire diameters of 110 nm and 130 nm. Fig.6(b) indicates the influence of different nanowire spacing on the resonance peak. When the nanowire spacing increases, energy will leak from the nanowire gap to the analyte, resulting in the reduction of light energy in the plasma material and lower confinement loss. It can be seen from Fig.6(b) that when the nanowire spacing is 40 nm, the sensor performance is the best.

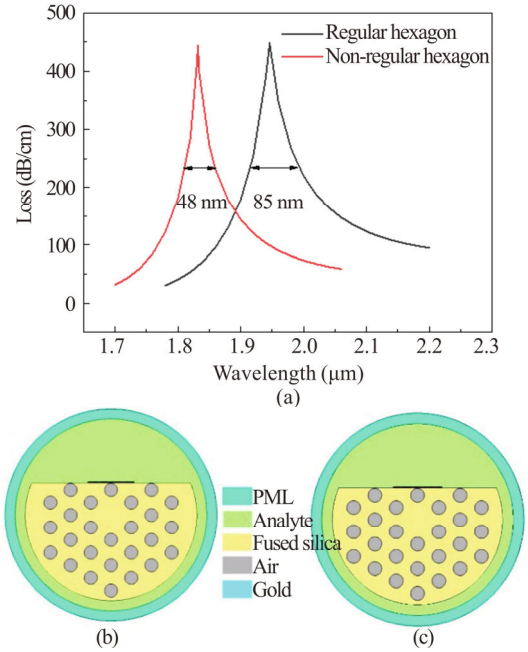

Fig.5 (a) Comparison of loss peaks between different arrangement of air holes: (b) Regular hexagonal structure; (c) Non-regular hexagonal structure

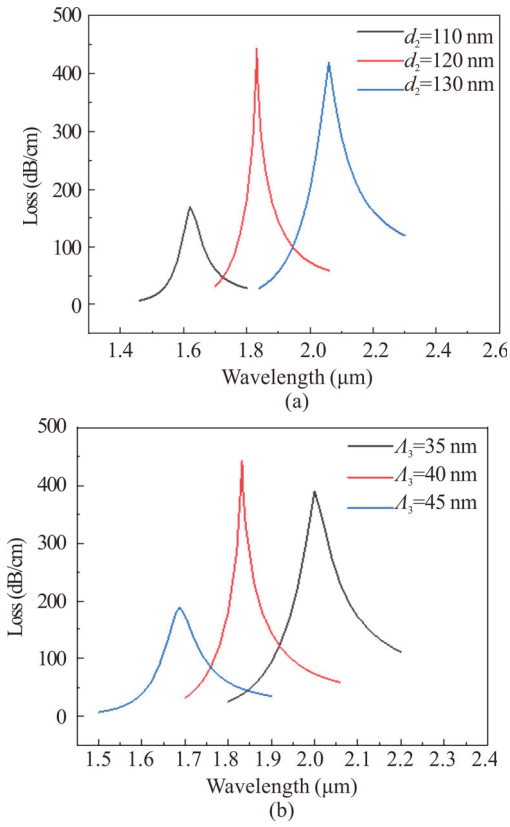

Fig.6 Variation of loss peak with (a) the nanowire diameter and (b) the nanowire spacing

Fig.7 shows the influence of the distance from the fiber center to the polished surface on the loss peak. It can be seen that when the distance from the surface is 3.2 μm, the sensor will get narrower *FWHM* and higher confinement loss. The possible reason may be that the distance of energy propagation in the *y* direction is shortened, so that more energy propagates to the surface of plasma material, resulting in stronger LSPR phenomenon. When *H*=3.15 μm, the upper air holes are tangent to the surface. The possible reason for the sharp reduction of confinement loss is that the upper air holes block the energy propagation to the plasma material in the middle region, resulting in LSPR effect only occurs on both sides of silver nanowires.

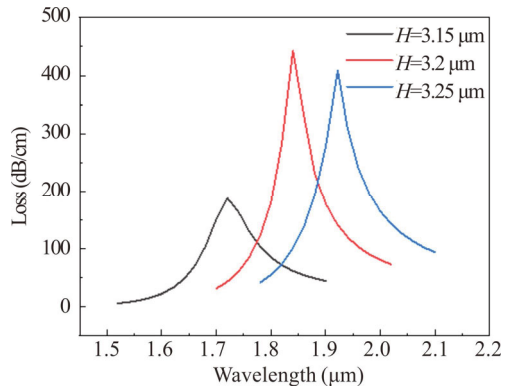

Fig.7 Variation of loss peak with the distance from fiber center to the polished surface

Fig.8(a) shows the shift of resonance wavelength when the refractive index of analyte changes from 1.26 to 1.33. The wavelength sensitivity of the sensor can be calculated by[15]

$$S_{\lambda}\,(\mathrm{nm/RIU}) = \frac{\Delta\lambda_{\mathrm{peak}}}{\Delta n_{\mathrm{a}}}, \tag{5}$$

where $\Delta\lambda_{\mathrm{peak}}$ is the shift of resonance wavelength, and Δn_{a} is the change in the refractive index of the analyte. The average sensitivity of the sensor is 12 460 nm/RIU when the refractive index range of the analyte is 1.30—1.33, and the maximum sensitivity is 16 400 nm/RIU when the refractive index of analyte is 1.33. Fig.8(b) shows the second-order fitting curve between the resonance wavelength and the refractive index of the analyte. The adjusted *R*-square value of this fitting is 0.997 67, which indicates that the fitting is consistent.

As shown in Tab.1, our study has achieved higher sensitivity than other sensors in the detection of low refractive index analytes.

In this paper, we have proposed and simulated a sensor with 31 silver nanowires regularly arranged on the surface of the D-shaped PCF. Through the adjustment of various parameters of the sensor, we obtained the fiber structure suitable for the detection of low refractive index analyte. The refractive index detecting range is from 1.26 to 1.33, and the maximum wavelength sensitivity

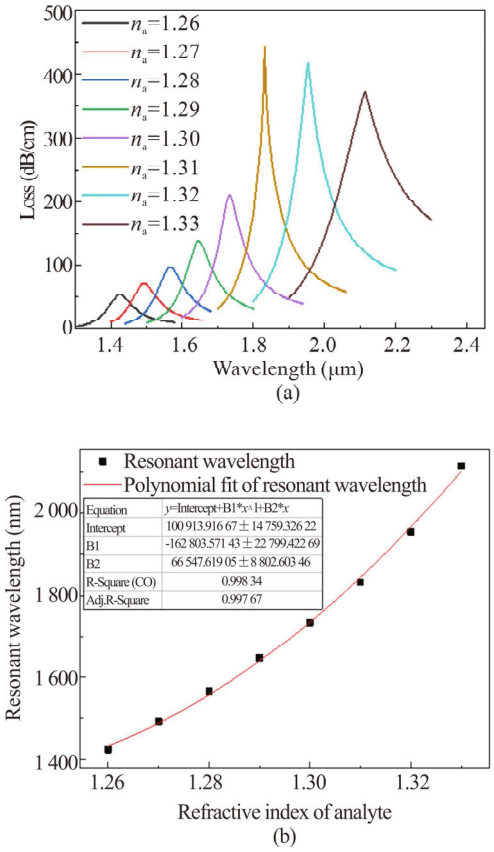

Fig.8 (a) Loss peaks of the proposed sensor for different analyte refractive indexes; (b) Variation of resonance wavelength with analyte refractive index changing from 1.26 to 1.33

Tab.1 Comparison with other sensors

References	Refractive index range	Maximum sensitivity (nm/RIU)	Maximum sensitivity below 1.33 (nm/RIU)
[16]	1.12—1.36	17 500	8 000
[17]	1.27—1.365	72 000	5 000
[18]	1.33—1.41	*X*-pol: 16 000 *Y*-pol: 17 000	-
[19]	1.33—1.44	12 530	2 694.3
[20]	1.30—1.412	50 000	2 000
This paper	1.26—1.33	16 400	16 400

can reach 16 400 nm/RIU. This study realizes the high sensitivity detection of low refractive index analytes, and the simple arrangement of nanowires also makes the experiment easier.

Statements and Declarations

The authors declare that there are no conflicts of interest related to this article.

References

[1] GANGWAR R K, SINGH V K. Highly sensitive surface plasmon resonance based D-shaped photonic crystal fiber refractive index sensor[J]. Plasmonics, 2017, 12：1367-1372.

[2] JING J, WANG Q, WANG B. Refractive index sensing characteristics of carbon nanotube-deposited photonic crystal fiber SPR sensor[J]. Optical fiber technology, 2018, 43：137-144.

[3] YANG M, LONG S, ZHU W, et al. Design and optimization of nano-column array based surface plasmon resonance sensor[J]. Optical and quantum electronics, 2017, 49：31.

[4] LUAN N, WANG R, YAO J. Surface plasmon resonance sensor based on exposed-core microstructured optical fibers[J]. Electronics letters, 2015, 51(9)：714-715.

[5] LUAN N, YAO J. Surface plasmon resonance sensor based on exposed-core microstructured optical fiber placed with a silver wire[J]. IEEE photonics journal, 2016, 8(1)：1-8.

[6] ZHAO J, CAO S, LIAO C, et al. Surface plasmon resonance refractive sensor based on silver-coated side-polished fiber[J]. Sensors and actuators B：chemical, 2016, 230：206-211.

[7] FU H W, ZHANG M, DING J J, et al. A high sensitivity D-type surface plasmon resonance optical fiber refractive index sensor with graphene coated silver nano-columns[J]. Optical fiber technology, 2019, 48：34-39.

[8] WANG G Y, LU Y, DUAN L C, et al. A refractive index sensor based on PCF with ultra-wide detection range[J]. IEEE journal on selected topics in quantum electronics, 2021, 27：1-8.

[9] ZHANG W, LIAN Z G, TREVOR B, et al. A refractive index sensor based on a D-shaped photonic crystal fiber with a nanoscale gold belt[J]. Optical and quantum electronics, 2018, 50：29.

[10] LIU C, YANG L, LU X, et al. Mid-infrared surface plasmon resonance sensor based on photonic crystal fibers[J]. Optics express, 2017, 25：14227-14237.

[11] WANG J, LIU C, WANG F, et al. Surface plasmon resonance sensor based on coupling effects of dual photonic crystal fibers for low refractive indexes detection[J]. Results in physics, 2020：103240.

[12] SHARMA A K, GUPTA B D. On the performance of different bimetallic combinations in surface plasmon resonance based fiber optic sensors[J]. Journal of applied physics, 2007, 101(9Pt1)：299.

[13] LIU Y C, LI S G, et al. Surface plasmon resonance induced high sensitivity temperature and refractive index sensor based on evanescent field enhanced photonic crystal fiber[J]. Journal of lightwave technology, 2019, 38(4)：919-928.

[14] PANDEY A K, SHARMA A K. Simulation and analysis of plasmonic sensor in NIR with fluoride glass and graphene layer[J]. Photonics and nanostructures-fundamentals and applications, 2018, 28：94-99.

[15] PAUL A K, SARKAR A K, KHALEQUE A. Dual-core photonic crystal fiber plasmonic refractive index sensor：a numerical analysis[J]. Photonic sensors, 2019, 9(2)：11.

[16] WANG J, LIU C, WANG F, et al. Surface plasmon resonance sensor based on coupling effects of dual photonic crystal fibers for low refractive indexes detection[J]. Results in physics, 2020：103240.

[17] YANG H, WANG G, LU Y, et al. Highly sensitive refractive index sensor based on SPR with silver and titanium dioxide coating[J]. Optical and quantum electronics, 2021, 53(6)：341.

[18] ISLAM M R, JAMIL M A, ZAMAN S U, et al. Design and analysis of birefringent SPR based PCF biosensor with ultra-high sensitivity and low loss[J]. Optik-international journal for light and electron optics, 2020, 221：165311.

[19] LI B, ZHANG F, YAN X, et al. Numerical analysis of dual-parameter optical fiber sensor with large measurement range based on surface plasmon resonance[J]. IEEE sensors journal, 2021, 21(9)：10719-10725.

[20] MOLLAH M A, ISLAM M S. Novel single hole exposed-suspended core localized surface plasmon resonance sensor[J]. IEEE sensors journal, 2021, 21(3)：2813-2820.